International Journal of Nanomedicine

Dovepress
open access to scientific and medical research

Open Access Full Text Article

ORIGINAL RESEARCH

Durable antibacterial and UV-protective Ag/TiO_2@ fabrics for sustainable biomedical application

This article was published in the following Dove Press journal:
International Journal of Nanomedicine
31 March 2017
Number of times this article has been viewed

Shuhui Li
Tianxue Zhu
Jianying Huang
Qingqing Guo
Guoqiang Chen
Yuekun Lai

National Engineering Laboratory for Modern Silk, College of Textile and Clothing Engineering, Soochow University, Suzhou, People's Republic of China

Abstract: A facile method was developed to endow cotton fabric with remarkable antibacterial and ultraviolet (UV)-protective properties. The flower-like TiO_2 micro-nanoparticles were first deposited onto cotton fabric surface via hydrothermal deposition method. Then, the Ag NPs with a high deposition density were evenly formed onto TiO_2@cotton surface by sodium hydroxide solution pretreatment and followed by in situ reduction of ANO_3. This work focused on the influence of different hydrothermal reaction durations and the concentration of $AgNO_3$ on antibacterial activity against relevant microorganisms in medicine as well as on the UV-blocking property. Ag NPs-loaded TiO_2@cotton exhibited high antibacterial activity with an inhibition rate higher than 99% against *Staphylococcus aureus* and *Escherichia coli* bacteria. Moreover, the as-prepared cotton fabric coated with Ag NPs and TiO_2 NPs demonstrated outstanding UV protective ability with a high ultraviolet protection factor value of 56.39. Morphological image of the cells revealed a likely loss of viability as a result of the synergistically biocidal effects of TiO_2 and Ag on attached bacteria. These results demonstrate a facile and robust synthesis technology for fabricating multifunctional textiles with a promising biocidal activity against common Gram-negative and Gram-positive bacteria.

Keywords: TiO_2 nanoparticles, Ag nanoparticles, fabric, antibacterial, UV-shielding, biomedical

Introduction

With the development of social technology and the improvement of standard of life, commercial, common textiles cannot cater to the need of consumers and market, especially for cotton fabric, which are regarded as the most abundant and widely used natural renewable cellulose materials. Despite the excellent properties of cellulose surface, some inherent features such as being hydrophilic, vulnerability to bacteria and microorganisms, inferior chemical and thermal stability, and poor persistence to ultraviolet (UV) radiation inhibited its wide application in advanced fields.[1–7] Recently, more and more literature about preparing high-technology textiles using nanotechnology have been reported.[8–18] New properties were imparted to enhance the added value of finished products. Ag and TiO_2 nanomaterials are widely applied to many consumer products and biomedical purposes due to their unique properties in UV protection, antibacterial and photocatalytic activity, biocompatibility, and great physicochemical stability.[19–26] Recently, Ag nanoparticles (NPs)-related fabrics have received great attention as topical dressings to prevent wound infection.

However, only few topical dressing products involve the use of Ag in the NP form. Moreover, among natural textile fibers used as wound dressing, cotton has attracted the greatest attention in literature for the construction of biocidal fabrics. Generally, monodisperse Ag NPs can be obtained by chemical reduction,[27,28] electrochemical,[29–31] photochemical,[32,33] and sonochemical,[34–36] as well as using pulsed laser deposition.[37,38]

Correspondence: Guoqiang Chen; Yuekun Lai
National Engineering Laboratory for Modern Silk, College of Textile and Clothing Engineering, Soochow University, No 199 Ren'ai Road, Suzhou 215123, People's Republic of China
Tel +86 512 6706 1109
Email yklai@suda.edu.cn; chenguojiang@suda.edu.cn

submit your manuscript | www.dovepress.com
Dovepress
http://dx.doi.org/10.2147/IJN.S132035

Among these methods, the chemical reduction is one of the most commonly used technologies. However, NPs obtained by chemical deposition method are prone to be scratched under mechanical external force. This work aims to propose a differently modified TiO_2@fabric substrate in combination with the firm immobilization of Ag in the form of NPs. In order to deal with the difficulty of inferior stability and mechanical strength of fabricated nanoparticles, in the current study, we rationally designed and fabricated robust flower-like hierarchical TiO_2 particles on cotton substrate first and then fixed Ag NPs onto TiO_2 coating surface to improve the binding strength. The results showed excellent UV-protective property and remarkable antibacterial activity against *Escherichia coli* and *Staphylococcus aureus*, with an inhibition rate above 99%.

Experimental work

Materials and regents

Potassium titanium oxalate was obtained from Titanchem Co. Ltd. (Shanghai, People's Republic of China); diethylene glycol was supplied by Shanghai J&K Scientific Co. Ltd. (Beijing, People's Republic of China); raw cotton fabric was purchased from a local store (Suzhou, People's Republic of China); sodium hydroxide (NaOH, AR) was supplied by Sinapharm Chemical Reagent Co. Ltd. (Shanghai, People's Republic of China); $AgNO_3$ was purchased from Shanghai Aladdin Industrial Corporate (Shanghai, People's Republic of China).

Preparation of TiO_2@cotton

The fabrication of hierarchical TiO_2@cotton fabric has been detailed in our previous study (Scheme 1).[39] Briefly, 0.75 g (2 mM) of potassium titanium oxalate was dissolved in deionized water (15 mL), then sonicated for 5 min in an ultrasonic cleaning machine (KQ100E; Kunshan Ultrasonic Instrument Co., Ltd., Kunshan City, People's Republic of China) with a frequency of 40 kHz, followed by adding diethylene glycol (20 mL) under vigorous magnetic stirring. After stirring for 20 min, the mixed solution was transferred into a teflon-lined stainless steel vessel (100 mL). The cleaned cotton were immersed into the mixed solution and then allowed to react for 5 h and 10 h with the hydrothermal treatment temperature at 150°C. After the hydrothermal reaction was completed, the cotton pieces were thoroughly washed with deionized water to remove the residual reactants and dried at 70°C in vacuum oven. Since the treated temperatures are the same, we called the as-prepared TiO_2@cotton as TiC(t) for the convenience consideration, which the item "t" represents the reaction duration. For example, the TiC(5) represents TiO_2@cotton fabric with the reaction temperature of 150°C and hydrothermal treatment time of 5 h.

In situ growth of Ag NPs on TiO_2@cotton surface

The in situ growth of Ag NPs on TiO_2@cotton surface was obtained by immersing the as-prepared TiO_2@cotton into 6 M NaOH solution for 5 min to activate the hydrophilic groups, followed by transferring into various concentrations (6.25 mM, 12.5 mM, 25 mM, 50 mM, and 100 mM) of $AgNO_3$ solution for 30 min reaction in the dark (Scheme 1). After the reaction, the samples were washed with deionized water in order to remove excess reactants. Subsequently, the cotton samples were soaked in different concentrations of

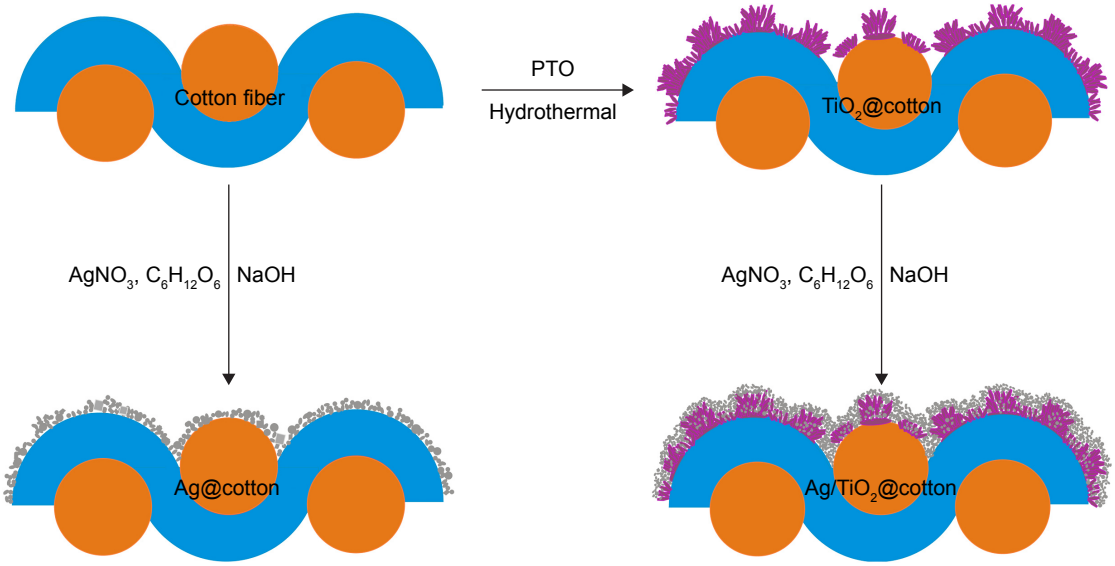

Scheme 1 The synthesis of TiO_2 flower-like micro-NPs and Ag NPs coated onto cotton fabric.
Abbreviations: NP, nanoparticle; PTO, potassium titanium oxalate.

reducing glucose solution for preparing various Ag/TiO_2@ cotton fabrics. It should be noted that the obtained Ag/TiO_2@ cotton with various $AgNO_3$ concentrations is recorded as AgTiC(t)-X, in which the "X" represents the concentration of $AgNO_3$ solution.

Antibacterial test

The antibacterial activity experiments were conducted against *E. coli* and *S. aureus* according to the agar diffusion plate method (GB/T 20944.3-2008) and the shake flask method (GB/T 20944.1-2007). The agar diffusion plate method provides qualitative data (inhibition zone) for measuring the antibacterial activity of as-prepared coatings, while the shake flake method shows quantitative data for the inhibition rate in number of colonies formed, converted by the average colony forming units per milliliter of buffer solution in the flask (CFU/mL). The inhibition zone test and the inhibition rate test are regarded as two parameters to characterize the antibacterial effect of samples. The specific process of inhibition zone experiment was as follows: a single colony from the corresponding bacterial cultures was used for the preparation of *S. aureus* and *E. coli* suspensions. The culture was then incubated at 37°C and 150 rpm and grown overnight in sterile nutrient broth. The inoculated bacterial culture was diluted with sterile phosphate-buffered saline (PBS) solution (pH 7.4) to 10^4 times, 10^5 times, and 10^6 times the original bacterial concentration. One hundred microliters of each diluted bacterial suspension was added dropwise onto fresh solidified agar and the bacterial suspension was spread evenly with triangular glass ring. Each of the Ag/TiO_2-coated cotton and uncoated Ag NPs TiO_2@cotton as well as cotton fabric with the same size (1 cm^2) was placed onto and intensely contacted with the agar that has a uniform bacterial suspension layer on surface. These plates were further incubated at 37°C in an incubator for 18–24 h.

For the inhibition rate experiment, the inoculated bacteria diluted to 10^6 times of the original concentration were used in the whole culture process since the number of bacteria in this condition was about 1×10^8–5×10^8 CFU/mL. The as-prepared cotton fabric pieces (375 mg) were cultured with 35 mL PBS solution and 2.5 mL diluted bacteria (10^6 times) at 24°C and 150 rpm overnight. After incubating for a certain period, the bacterial cells that survived were quantitatively assayed by standard plate count method. Briefly, after an incubation period of 24 h at 24°C, 1 mL of cultured bacteria were diluted to 10^6 times of the original concentration in sterile PBS solution and cultured in agar plate at 37°C for 24 h, and then the colonies were counted to determine the bacterial cells that survived. The antibacterial efficiency is given as the percentage of bacterial reduction by calculating the ratio between the number of survival bacteria before (A) and after (B) contact with fabrics using the following equation:

$$\text{Bacterial reduction } (\%) = \frac{A - B}{A} \times 100\%. \quad (1)$$

For scanning electron microscope (SEM) observation, 60 µL bacterium solution with the concentration of 10^7 CFU/mL was seeded on the sample surface, incubated at 37°C for 4 h, fixed with 2.5 vol% glutaraldehyde solution overnight at 4°C, and then washed with sterile PBS three times, each time for 15 min. Finally, the sample was dehydrated in graded ethanol (30, 50, 70, 85, 90, and 100 vol/vol%) for 10 min in each concentration. Subsequently, samples were vacuum-dried at 60°C overnight followed by coating gold before SEM observation.

Characterization of the as-prepared coatings

The surface morphologies of TiO_2@cotton fabrics were characterized by a field emission scanning electron microscope (FESEM, Hitachi-S4800, Tokyo, Japan). Energy dispersive X-ray (EDX) spectrometer fit to TM3030 scanning electron microscope was applied for elemental analysis. All samples were coated by gold sputtering prior to SEM observations. Fourier transform infrared (FTIR) analysis was conducted on a Nicolet 5700 FT-IR spectrometer equipped with a single reflection attenuated total reflectance system. The spectra were recorded from 400 cm^{-1} to 4,000 cm^{-1}, with a resolution ratio of 4 cm^{-1}. X-ray photoelectron spectroscopy (XPS) spectra were obtained by using a Kratos Axis Ultra HAS X-ray photoelectron spectroscopy with an Al Ka X-ray source at a reduced power of 100 W. The vacuum pressure in the analysis chamber was maintained at 4.0×10^{-9} Pa. The binding energies (BEs) were normalized to the signal for adventitious C 1s at 284.5 eV. The step size for high-resolution scan was 0.1 eV, and the pass energy was 80 eV. Anti-UV properties of fabric sample were measured by Labsphere UV-1000F Ultraviolet Transmittance Analyzer at the wavelength of 250–450 nm. The laundering durability of coated cotton fabric was assessed using a washing fastness tester (SW-12A; Wuxi Textile Machinery Co., Ltd., Wuxi, People's Republic of China) according to American Association of Textile Chemists and Colourists (AATCC 61-2006) standard method under 2A condition using a 0.15% standard reference detergent without optical brightener and 50 stainless steel balls. One accelerated laundering durability test is equal to five commercial or domestic laundering cycles.

Results and discussion

The effect of surface morphologies

The surface morphologies of pristine cotton, TiO_2@cotton, Ag@cotton, and Ag/TiO_2@cotton were characterized by SEM. The pristine cotton surface is smooth with some grooves embedded in fiber as shown in Figure 1A. After hydrothermal reaction, numerous flower-like TiO_2 particles were found to coat the cotton surface, and these had a diameter range from 0.02 to 0.5 μm (Figure 1B). In addition, such flower-like TiO_2 microparticles consisted of large amount of TiO_2 nanorods, and numerous nanoscale particles with preferential orientation were formed onto fiber surface as hydrolysis and condensation reactions proceeded, which became flower-shaped clusters. Meanwhile, as the treatment duration increased, TiO_2 particles tended to aggregate, and finally a uniform and compact flower-like hierarchical micro/nanostructure TiO_2 particles film was formed on the cotton fiber surface. Ag NPs with an average size of 20–200 nm were in situ grown on cotton and TiO_2@cotton surface. The scale of Ag NPs on pristine cotton was a little large in comparison with that of TiO_2@cotton surface and some of them were accumulated together forming composite particles (Figure 1C). Compared with pristine cotton fiber surface, flower-like hierarchical TiO_2 micro/NP structure morphology was more beneficial for the imbibition of Ag nanoparticles. As a result, evenly smaller scale (<50 nm) Ag NPs were embedded into hierarchical TiO_2 micro-nanostructure, other big-scale Ag NPs (>100 nm) were located on flower-like TiO_2 NPs (Figure 1D). We have also investigated the effect of the $AgNO_3$ concentrations on surface morphologies (Figure S1).

EDS analysis

The chemical composition of Ag/TiO_2@cotton was characterized by EDS measurement. From the EDS spectrum mappings and the EDS spectra of Ag/TiO_2@cotton (Figure 2A–F), we observed that the as-prepared sample mainly consisted of C, O, Ti, Ag, and Au elements. The presence of Au element is caused by sputtering metallic gold to improve conductivity of cotton cellulose surface. However, the component atoms on pristine cotton are determined to be C and O elements

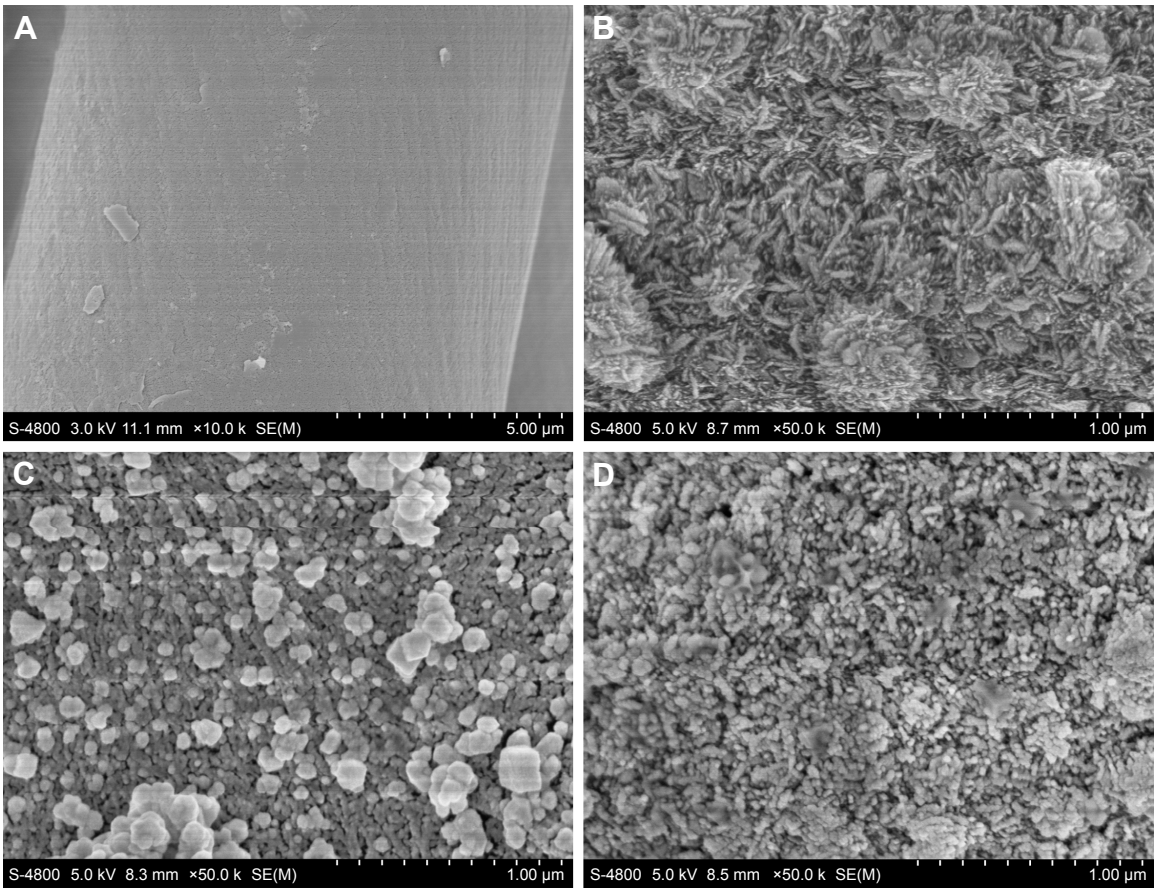

Figure 1 SEM images of various cotton fabrics.
Notes: (**A**) Pristine cotton, (**B**) TiC(5), (**C**) AgC-100, (**D**) AgTiC(5)-100.
Abbreviation: SEM, scanning electron microscopy.

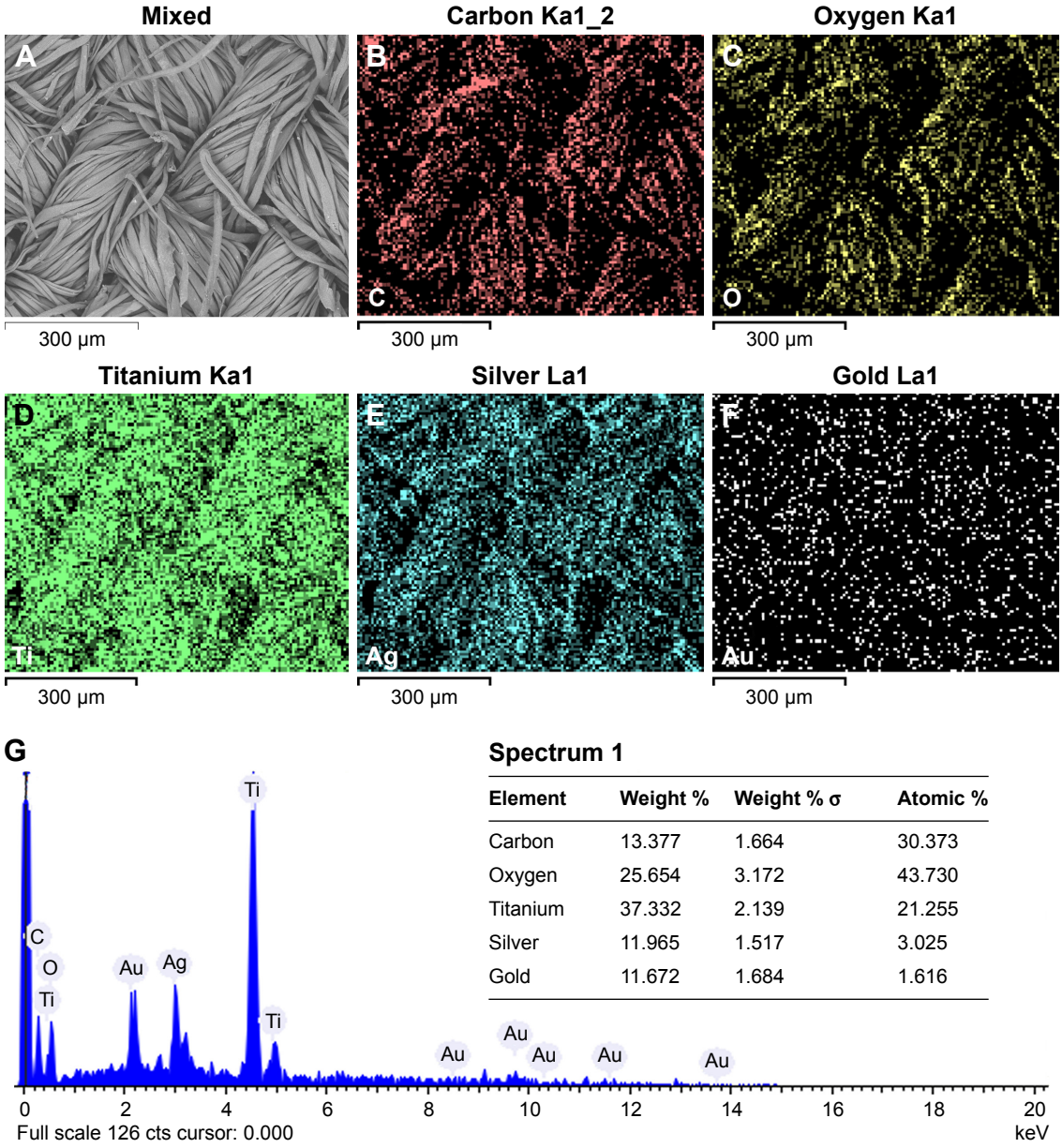

Figure 2 Elements mapping (**A**–**F**) and the energy spectrum and elements proportion (**G**) of AgTiC(5)-100 sample surface.

(Figure S2). Therefore, the results confirmed that TiO_2 and Ag NPs were successfully formed on cotton fiber surface. The EDS spectrum mapping of Ti and Ag elements indicated TiO_2 and Ag NPs evenly distributed on cotton surface. The relative atom ratio of C/O/Ti/Ag/Au was about 30.373/43.370/21.255/3.025/1.616% (Figure 2G).

FTIR and XPS analyses

FTIR analysis showed that there were no significant changes on various cotton surfaces, demonstrating that there is no new functional group formation during the fabrication process with the flower-like TiO_2 NPs and Ag NPs deposition onto cotton fiber surface (Figure 3A). Although the chemical structure and chemical bond before and after modification of cotton did not appear to have changed, the surface morphologies and chemical elements changed. The surface chemical composition of cotton fabric before and after hydrothermal treatment and in situ reduction of $AgNO_3$ was further confirmed by XPS. Figure 3B–D showed the wide scan and high-resolution XPS spectra of Ti 2p and Ag 3d on various coating cotton surfaces. Compared with the blank cotton surface, two new characteristic peaks at BEs of 455 eV and 371 eV were found (as shown in Figure 3B). The curved fit of Ti 2p core-level XPS spectrum was composited of two distinct peaks at BEs of 458.4 eV and

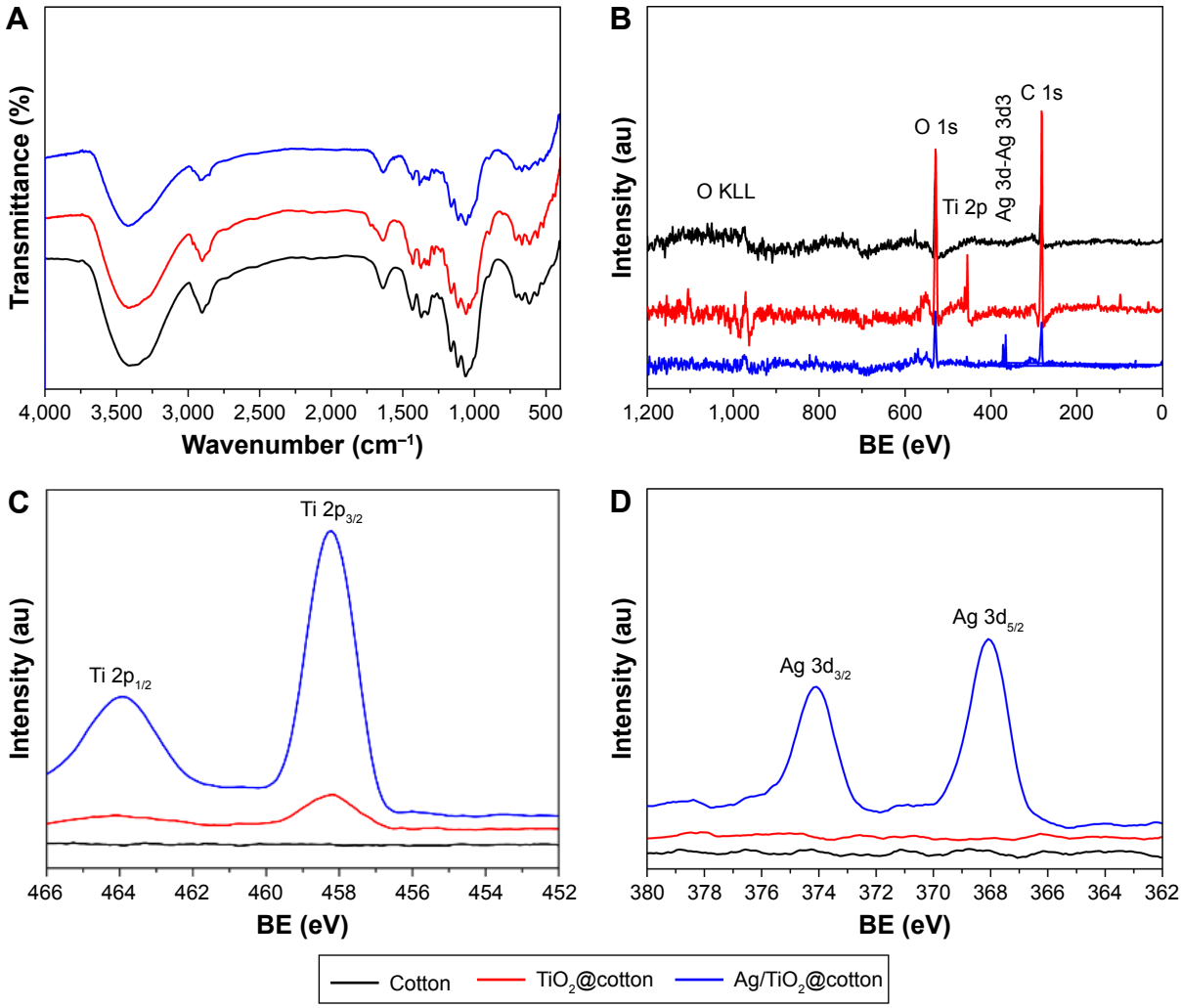

Figure 3 (**A**) FTIR spectra and (**B**) XPS spectra of cotton fabric before and after hydrothermal treatment and in situ deposition of Ag NPs. Corresponding high-resolution XPS spectra of Ti 2p (**C**) and Ag 3d (**D**).
Abbreviations: au, absorbance unit; BE, binding energy; FTIR, Fourier transform infrared; NPs, nanoparticles; XPS, X-ray photoelectron spectroscopy.

464.2 eV assigned for Ti $2p_{1/2}$ and Ti $2p_{3/2}$, respectively. The splitting energy about 5.8 eV between Ti $2p_{1/2}$ and Ti $2p_{3/2}$ indicated the existence of Ti^{4+}, which is in agreement with the reported result for TiO_2.[40] Two special characteristic peaks at BEs of 368.2 eV and 374.2 eV assigned to Ag $3d_{5/2}$ and Ag $3d_{3/2}$ appeared on Ag/TiO_2@cotton sample. The splitting energy of about 6.0 eV between them demonstrated Ag (0) NPs successfully coated on TiO_2@cotton surface. These results were consistent with the analysis of EDS spectrum, and they all demonstrated that flower-like TiO_2 particles and Ag NPs immobilized onto cotton surface.

Antibacterial experiment

TiO_2 particles and Ag NPs as excellent antibacterial agents are widely applied in the UV protection and antibacterial field. To investigate the antibacterial activity of TiO_2 NPs- and Ag NPs-coated cotton fabric, we chose the Gram-positive bacteria (*S. aureus*) and the Gram-negative bacteria (*E. coli*) as target bacteria. In our research, the qualitative measurement method – inhibition zone test against *S. aureus* bacteria and inhibition rate experiment which is regarded as a quantitative technology against *E. coli* and *S. aureus* – were conducted. Figure 4A and B showed inhibition zone of untreated cotton and TiO_2 NPs and Ag NPs cotton fabric. Unlike the pristine cotton and TiO_2@cotton, Ag NPs-coated TiO_2@cotton reduced with different concentrations of $AgNO_3$ exhibited excellent antibacterial activity, with inhibition zone sizes ranging from 1 to 1.2 cm. The reason for untreated cotton not having inhibition zone is the absence of any antibacterial agents on cotton fiber structure. However, no apparent inhibition zone appeared on TiO_2 NPs-coated cotton because the antibacterial activity of anatase TiO_2 NPs needed to be stimulated by irradiation during the incubation process. In order to quantitatively analyze the bacterial reduction on

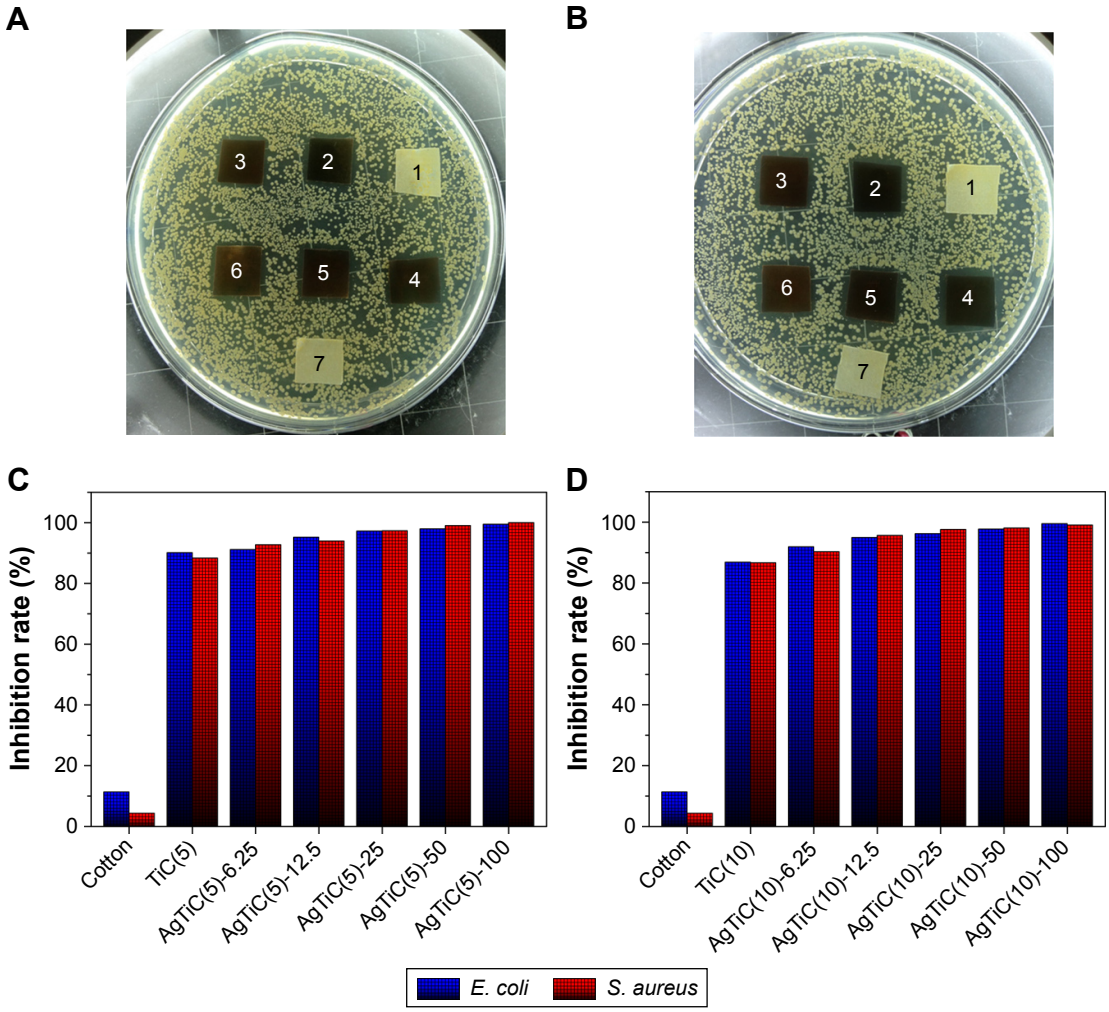

Figure 4 The inhibition zone and inhibition rate of various samples: the numbers 1–7 represent TiO_2@cotton depositing for 5 h (**A**) and 10 h (**B**), in situ growth of Ag NPs on TiO_2@cotton with various $AgNO_3$ concentrations including 6.25 mM, 12.5 mM, 25 mM, 50 mM, 100 mM, and pristine cotton, respectively. Corresponding inhibition rates against *E. coli* and *S. aureus* on various samples (**C**, **D**).
Abbreviations: *E. coli*, *Escherichia coli*; NP, nanoparticle; *S. aureus*, *Staphylococcus aureus*.

TiO_2 NPs-coated cotton surface and Ag and TiO_2 NPs-coated cotton surface, the inhibition rate experiments against *E. coli* and *S. aureus* were done among various samples. The whole incubation process for shaking flask at 24°C was under irradiation condition. As expected, the pristine cotton demonstrated a poor antibacterial activity against both *E. coli* and *S. aureus*, with inhibition rate value of 11.39% and 4.37%, respectively. For TiC(5), the bacterial reduction rate was beyond 86% against *E. coli* and *S. aureus* (Figure 4C). In addition, the inhibition rate rose with the increasing hydrothermal deposition duration (Figure 4D). Ag NPs have a significant influence on bacterial reduction; even a small dosage of Ag NPs induced the inhibition rate to increase to above 90%. When the concentration of $AgNO_3$ increased, the antibacterial activity against *E. coli* and *S. aureus* improved slowly and stably. Similar phenomenon was observed at TiC(10) and AgTiC(10) at different concentrations of $AgNO_3$ samples.

UV-blocking property

Ultraviolet protection factor (UPF) is a significant parameter to measure UV-shielding ability fabric. The UPF value is the ratio of UV radiation average effect when the skin is unprotected compared with that when the skin is protected with a protective product. It can be determined by the following equation:[41]

$$\mathrm{UPF} = \frac{\sum_{280\ \mathrm{nm}}^{380\ \mathrm{nm}} E_\lambda S_\lambda \Delta_\lambda}{\sum_{280\ \mathrm{nm}}^{380\ \mathrm{nm}} E_\lambda S_\lambda T_\lambda \Delta_\lambda} \quad (2)$$

where E_λ is the relative erythemal spectral effectiveness; S_λ is the solar spectral irradiance; T_λ is the average spectral transmission of the specimen; and Δ_λ is the measured wavelength interval (nm). The UPF value is calculated automatically

according to the UPF standard Australia/New Zealand standard AS/NZS 4399:1996.

TiO_2 NPs have strong UV absorbance ability and are often used as UV-blocking agents. As can be seen from Figure 5, the UV transmission properties of untreated cotton and TiO_2 NPs- and Ag NPs-coated cotton were measured at wavelength range from 250 to 450 nm. Moreover, Table 1 gives the UPF values and the percentages of UV transmittance at wavelength range from 320 to 400 nm for UVA and UVB (280–320 nm). The results indicated that the pristine cotton has a poor UV-shielding ability with an extremely low UPF value since the cellulose cotton cannot absorb UV radiation. It was very extraordinary that excellent UV-protection property against UV radiation for TiO_2-coated cotton was observed, especially for the cotton samples coated with a thicker TiO_2 NPs film after a longer deposition duration. Furthermore, all Ag NPs deposited on TiO_2@cotton samples exhibited better UV-blocking property than pristine cotton fabric and as-prepared TiO_2@cotton surface under the same treatment condition. All results imply that the effectiveness in UV shielding is not only caused by the high UV absorbance and scattering property of flower-like anatase TiO_2 NPs and Ag NPs, but also the gaps between the yarns can be filled with Ag and TiO_2 NPs during the coating process.[42–44] Importantly, a higher concentration of $AgNO_3$ reduced on a 10 h deposition duration of TiO_2@cotton surface provided a best UV-protection ability, with the UPF value raised up to above 50, a level corresponding to the UPF rating of 50+ (Table 1). Moreover, except for the cotton fabric, all the remaining samples exhibited significant UV-blocking property, and the UVA value of some treated samples was below 5%.

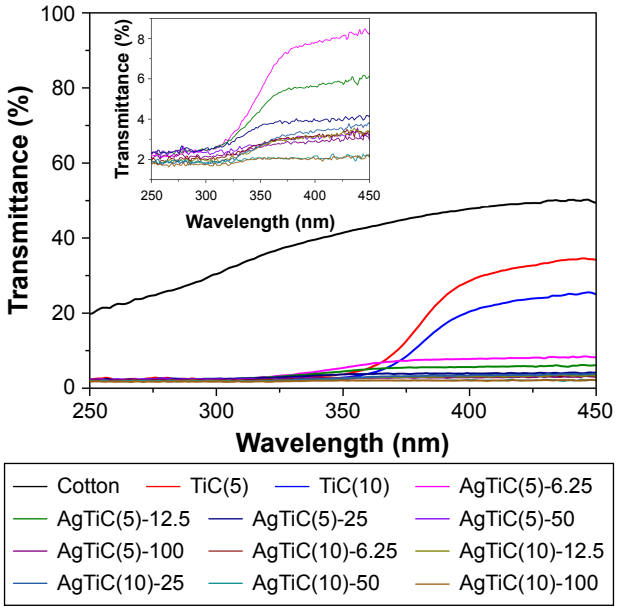

Figure 5 The UV transmittance property test of the pristine cotton and treated cotton with TiO_2 NPs and Ag NPs; inset is the UV transmittance curve of Ag NPs-coated TiO_2@cotton samples.
Abbreviations: NP, nanoparticle; UV, ultraviolet.

Table 1 The corresponding UPF, UVA, and UVB values of the original cotton and cotton coated with TiO_2 NPs and Ag NPs

Samples	UPF	UVA (%)	UVB (%)
Cotton	3.05	41.73	30.62
TiC(5)	34.60	9.89	2.50
TiC(10)	46.31	7.04	1.89
AgTiC(5)-6.25	35.16	5.44	2.55
AgTiC(5)-12.5	36.38	4.67	2.52
AgTiC(5)-25	38.43	3.46	2.48
AgTiC(5)-50	40.94	2.86	2.41
AgTiC(5)-100	44.41	2.67	2.21
AgTiC(10)-6.25	48.68	2.68	1.99
AgTiC(10)-12.5	50.67	2.54	1.94
AgTiC(10)-25	51.74	2.60	1.86
AgTiC(10)-50	53.81	1.97	1.86
AgTiC(10)-100	56.39	1.93	1.76

Abbreviations: NP, naoparticle; UPF, ultraviolet protection factor; UV, ultraviolet.

Stability of UV-protection ability

In order to investigate the UV-blocking property of coated cotton during practical application (such as washing), we conducted laundering experiments for 50 commercial cycles (equal to 10 cycles accelerated laundering) according to AATCC (61-2006) standard under 2A condition. The final

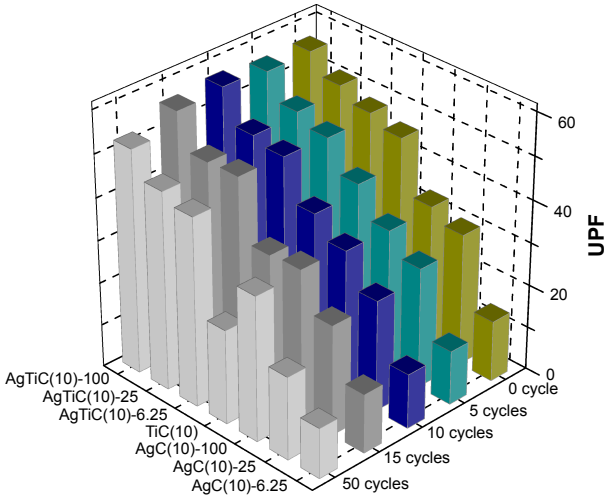

Figure 6 The stability of the TiC fabric, AgC fabric, and AgTiC fabric for UV-protection property before and after laundering numerous times according to AATCC 61-2006 standard under 2A condition.
Abbreviations: AATCC, American Association of Textile Chemists and Colourists; UPF, ultraviolet protection factor; UV, ultraviolet.

results of UV transmittance property on TiC, AgC, and AgTiC fabric are shown in Figure 6. From this histogram, we can observe the UPF value of TiC(10) almost decreased by half after 50 commercial cycles of laundering, which is attributed to the TiO_2 micro/NPs hierarchical structure that easily broke and was destroyed under mechanical force during washing process. However, the UPF values decreased little for AgC fabric, which displayed good, durable laundering ability. Moreover, the UPF of Ag NPs- and flower-like TiO_2 NPs-coated fabric after washing for 50 cycles just decreased 4.58% at an optimum condition in comparison with that of prior to washing. Though the UPF value was slightly decreased compared to before washing, high level UV protection was retained. This is mostly attributed to the formation of covalent bonding as a result of dehydration reaction between cellulosic hydroxyl group and hydroxyl group of TiO_2 after hydrothermal treatment. These results also suggested a strong adhesion, and these are confirmed by the results from the SEM observations (Figure S3).

Antibacterial activity after laundering

Furthermore, we conducted antibacterial activity experiments against *E. coli* on cotton fabric coated with different concentrations of NPs after 50 cycles of commercial laundering (Figure 7). After culturing in agar plate at 37°C for 24 h, the colonies were counted to determine the bacterial cells that survived. As expected, the number of bacterial colonies grown in the absence of any NP-coated cotton was the most (approximately 3.27×10^8 CFU/mL) (Figure 7B). However, the number of bacterial cells that survived on TiO_2 NPs-coated cotton surface reduced by an order of magnitude. Even Ag NPs-decorated cotton fabric displayed similar bacterial colonies, exhibiting a good antibacterial activity with an inhibition rate of 80.12% (Figure 7A). For TiO_2 and Ag composite NP-modified fabric surface, less surviving bacterial colonies were found, and with the increasing of the concentration of Ag, the bacterial number was decreased. Correspondingly, the inhibition rates of AgTiC samples were higher than TiC and AgC fabric surfaces. Moreover, a small dose of Ag (6.25 mM) can cause in excess of 80% inhibition of bacterial growth. With the Ag content increase, the inhibition effect became excellent. Compared with samples before laundering, the inhibition rate decreased 8% at most. The results clearly indicated that Ag and TiO_2 NPs were robust and cooperated with each other for resisting mechanical force during laundering cycles. Meanwhile, the excellent antibacterial activity of both endowed the whole cotton fabric with outstanding antibacterial ability.

Mechanism analysis of antibacterial property

The possible mechanism of antibacterial performance is discussed in this work (Scheme 2). The TiO_2-coated cotton exhibited good antibacterial performance compared with cotton blank. The most powerful interpretation is that TiO_2 coating may provide no substance for bacteria, whereas cellulose cotton surface offers good condition for bacterial growth and maintains good respiration due to its textured structure. The Ag NPs have excellent antibacterial activity

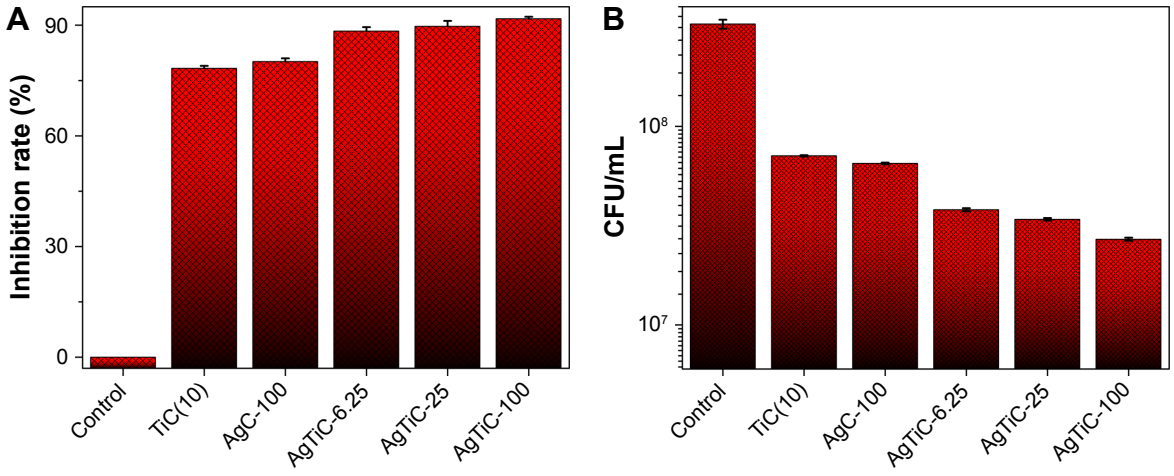

Figure 7 The inhibition rates (**A**) and number of survived bacterial colonies (**B**) of *E. coli* on various prepared cotton fabrics after 50 cycles of domestic laundering.
Abbreviation: *E. coli*, *Escherichia coli*.

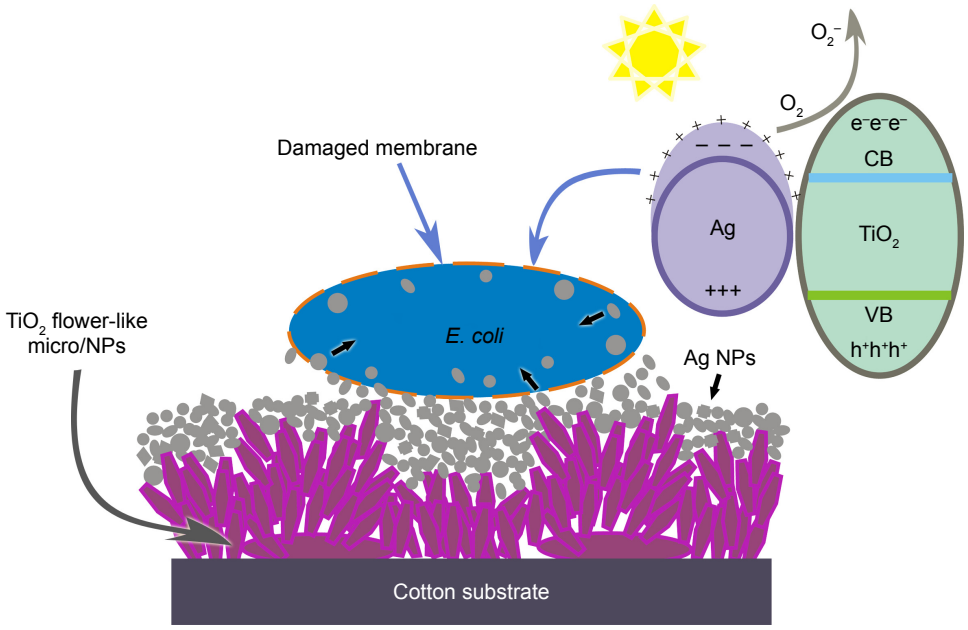

Scheme 2 The proposed mechanism of antibacterial activity on cotton surface coated with TiO_2 and Ag NPs.
Abbreviations: *E. coli*, *Escherichia coli*; NP, nanoparticle; CB, conduction band; VB, valence band.

since they have extremely large surface area which provides good contact with microorganisms. Ag NPs not only attach to bacteria cell but also penetrate inside the bacterial cell or membrane. After Ag NPs entered, bacteria would be killed by inhibition of its respiration process. For example, the presence of Ag NPs can inhibit the uptake of phosphate and the release of phosphate, mannitol, succinate, proline, and glutamine in *E. coli* cells. The NPs preferably break down the cell wall of the microorganism and attack the respiration chain and cell division, finally leading to the cell death.[45–47] In addition, metallic Ag reacts with moisture and gets ionized; the ionized Ag is highly active in comparison to metallic Ag. Especially under visible light, many reactive species ($\cdot O_2^-$, ·OH, photo-generated holes and electrons) are created on cellulose cotton surface. Actively ionized Ag destroys the cell wall structure and induces the lysis of bacteria cell, and finally bacteria are killed.[48] The NPs release Ag ions in the bacteria cell, which enhance the antibacterial activity.

SEM morphology of bacteria

In order to more intuitively describe antibacterial mechanism, the SEM morphology of bacteria was characterized to observe the membrane integrity after samples were incubated for 4 h at 37°C in a constant temperature incubator. As expected, more *E. coli* bacteria retaining their typical rod-like shape adhered on the pristine cotton surface, with an increase in growth leading to larger size and more number of organisms (Figure 8A and E). However, the bacteria adhered on TiO_2@cotton surface exhibited an obvious death-like state due to the crack in bacteria membrane (Figure 8B and F). These cell membranes displayed a flat and disintegrated appearance, which is consistent with the mechanism discussed in this work since the specific TiO_2 micro/NP coating can effectively inhibit the attachment or growth of bacterial. Compared with cotton blank, the bacteria exposed on Ag/cotton surface lose their cellular integrity, and apparent cell lysis was observed in the cell core, indicating bacteria cell damage and death (Figure 8C and G). A similar condition was found on bacteria of Ag/TiO_2@cotton. A majority of the cell membrane was destroyed and showed irregular appearance, which indicated bacteria have lost activity due to this breakage (Figure 8D and H). In addition, a minority of robust bacteria with intact membrane were seen as well. With the release of Ag NPs and Ag ions from antibacterial cotton surface, the bacteria were believed to have fully lost the cell wall structure, and so finally killed. The above results are in agreement with those discussed in the section on antibacterial mechanism.

Conclusion

We reported a facile route to fabricate multifunctional Ag/TiO_2@cotton fabrics with excellent antibacterial properties against common nosocomial bacteria and with UV-protection property. The TiO_2 and Ag NPs were uniformly dispersed throughout the fibers and were exclusively

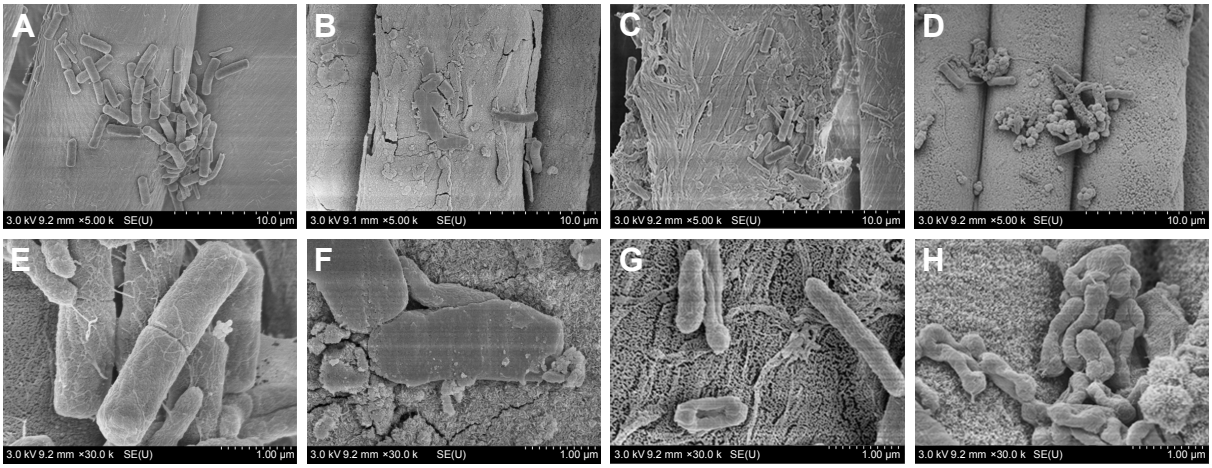

Figure 8 SEM morphology of *E. coli* bacteria adhered on various cotton fabric surfaces after incubating for 4 h (both low resolution and high resolution).
Notes: (**A**, **E**) Pristine cotton, (**B**, **F**) TiO_2@cotton, (**C**, **G**) Ag/cotton, (**D**, **H**) Ag/TiO_2@cotton.
Abbreviations: *E. coli*, *Escherichia coli*; SEM, scanning electron microscopy.

supported on the material surface. The flower-like hierarchical structure of TiO_2 NPs showed better UV shielding property due to their excellent UV absorbance and scattering abilities. The in situ synthesis of Ag NPs onto TiO_2@cotton surface not only improved the UPF values but also increased antibacterial activity against *E. coli* and *S. aureus*. The cotton fabric treated with TiO_2 NPs and Ag NPs also displayed sustainable bacterial reduction effect and durable UV-protection property before and after laundering. These results demonstrated that TiO_2 coating may not only act as a photocatalytic bacterial agent but also as a UV-shielding agent. This strategy is expected to be applied in various fabric surfaces to endow the pristine fabric with added value, and these multifunctional textiles have potential applications for use in UV shielding and antibacterial materials in biomedical applications.

Acknowledgments

The authors acknowledge the National Natural Science Foundation of China (51502185; 21501127), Natural Science Foundation of Jiangsu Province of China (BK20140400), Natural Science Foundation of the Jiangsu Higher Education Institutions of People's Republic of China (15KJB430025), Priority Academic Program Development of Jiangsu Higher Education Institutions (PAPD), and Jiangsu Province Annual Ordinary University Graduate Student Research and Innovation Project (provincial school assistant, KYLX16_0138) for financial support.

Disclosure

The authors report no conflicts of interest in this work.

References

1. Wang XF, Yu JY, Sun G, Ding B. Electrospun nanofibrous materials: a versatile medium for effective oil/water separation. *Mater Today*. 2016; 19(7):403–414.
2. Zhou XY, Zhang ZZ, Xu XH, et al. Robust and durable superhydrophobic cotton fabrics for oil/water separation. *ACS Appl Mater Interfaces*. 2013;5(15):7208–7214.
3. Zou HL, Lin SD, Tu YY, et al. Simple approach towards fabrication of highly durable and robust superhydrophobic cotton fabric from functional diblock copolymer. *J Mater Chem A*. 2013;1(37):11246–11260.
4. Nyström D, Lindqvist J, Östmark E, et al. Superhydrophobic and self-cleaning bio-fiber surfaces via ATRP and subsequent postfunctionalization. *ACS Appl Mater Interfaces*. 2009;1(4):816–823.
5. Li SH, Huang JY, Chen Z, Chen GQ, Lai Y. A review on special wettability textiles: theoretical models, fabrication technologies and multifunctional applications. *J Mater Chem A*. 2017;5(1):31–55.
6. Liu H, Gao SW, Cai JS, et al. Recent progress in fabrication and applications of superhydrophobic coating on cellulose-based substrates. *Materials*. 2016;9(3):124.
7. Liu Y, Pan YT, Wang X, et al. Effect of phosphorus-containing inorganic–organic hybrid coating on the flammability of cotton fabrics: synthesis, characterization and flammability. *Chem Eng J*. 2016;294:167–175.
8. Zhou H, Wang HX, Niu HT, Gestos A, Wang XG, Lin T. Fluoroalkyl silane modified silicone rubber/nanoparticle composite: a super durable, robust superhydrophobic fabric coating. *Adv Mater*. 2012;24(18): 2409–2412.
9. Zhao Y, Wang HX, Zhou H, Lin T. Directional fluid transport in thin porous materials and its functional applications. *Small*. 2017;13(4): 1601070.
10. Li J, Yan L, Tang XH, Feng H, Hu DC, Zha F. Robust superhydrophobic fabric bag filled with polyurethane sponges used for vacuum-assisted continuous and ultrafast absorption and collection of oils from water. *Adv Mater Interfaces*. 2016;3(9):1500770.
11. Xue CH, Li YR, Hou JL, Zhang L, Ma JZ, Jia ST. Self-roughened superhydrophobic coatings for continuous oil-water separation. *J Mater Chem A*. 2015;3(19):10248–10253.
12. Chen SS, Li X, Li Y, Sun JQ. Intumescent flame-retardant and self-healing superhydrophobic coatings on cotton fabric. *ACS Nano*. 2015;9(4):4070–4076.
13. Wu MC, Ma B, Pan TZ, Chen SS, Sun JQ. Silver-nanoparticle-colored cotton fabrics with tunable colors and durable antibacterial and self-healing superhydrophobic properties. *Adv Funct Mater*. 2016;26(4): 569–576.

14. Chen FX, Yang HY, Liu X, et al. Facile fabrication of multifunctional hybrid silk fabrics with controllable surface wettability and laundering durability. *ACS Appl Mater Interfaces*. 2016;8(8):5653–5660.
15. Li Y, Yang FF, Yu JY, Ding B. Hydrophobic fibrous membranes with tunable porous structure for equilibrium of breathable and waterproof performance. *Adv Mater Interfaces*. 2016;3(19):1600516.
16. Zhang SC, Liu H, Yu JY, Luo WJ, Ding B. Microwave structured polyamide-6 nanofiber/net membrane with embedded poly(m-phenylene isophthalamide) staple fibers for effective ultrafine particle filtration. *J Mater Chem A*. 2016;4(16):6149–6157.
17. Zhao H, Hou L, Lu YX. Electromagnetic shielding effectiveness and serviceability of the multilayer structured cuprammonium fabric/polypyrrole/copper (CF/PPy/Cu) composite. *Chem Eng J*. 2016;297:170–179.
18. Cao CY, Ge MZ, Huang JY, et al. Robust fluorine-free superhydrophobic PDMS-ormosil@fabrics for highly effective self-cleaning and efficient oil-water separation. *J Mater Chem A*. 2016;4(31):12179–12187.
19. Manna J, Goswami S, Shilpa N, Sahu N, Rana RK. Biomimetic method to assemble nanostructured Ag@ZnO on cotton fabrics: application as self-cleaning flexible materials with visible-light photocatalysis and antibacterial activities. *ACS Appl Mater Interfaces*. 2015;7(15):8076–8082.
20. Wang Q, Huang JY, Li HQ, et al. TiO_2 nanotube platforms for smart drug delivery: a review. *Int J Nanomedicine*. 2016;11:4819–4834.
21. Lai YK, Pan F, Xu C, Fuchs H, Chi LF. In situ surface-modification-induced superhydrophobic patterns with reversible wettability and adhesion. *Adv Mater*. 2013;25(12):1682–1686.
22. Liu X, Tian A, You J, et al. Antibacterial abilities and biocompatibilities of Ti-Ag alloys with nanotubular coatings. *Int J Nanomedicine*. 2016;11:5743–5755.
23. Montazer M, Keshvari A, Kahali P. Tragacanth gum/nano silver hydrogel on cotton fabric: in-situ synthesis and antibacterial properties. *Carbohyd Polym*. 2016;154:257–266.
24. Aladpoosh R, Montazer M, Samadi N. In situ green synthesis of silver nanoparticles on cotton fabric using Seidlitzia rosmarinus ashes. *Cellulose*. 2014;21(5):3755–3766.
25. Wang Q, Huang JY, Li HQ, et al. Recent advances on smart TiO_2 nanotube platforms for sustainable drug delivery applications. *Int J Nanomedicine*. 2017;12:151–165.
26. Ge MZ, Li QS, Cao CY, et al. One-dimensional TiO_2 nanotube photocatalysts for solar water splitting. *Adv Sci*. 2017;4(1):1600152.
27. Kruk T, Szczepanowicz K, Stefańska J, Socha RP, Warszyński P. Synthesis and antimicrobial activity of monodisperse copper nanoparticles. *Colloids Surf B: Biointerfaces*. 2015;128:17–22.
28. Ge MZ, Cao CY, Li SH, et al. In situ plasmonic Ag nanoparticle anchored TiO_2 nanotube arrays as visible-light-driven photocatalysts for enhanced water splitting. *Nanoscale*. 2016;8(9):5226–5234.
29. Reicha FM, Sarhan A, Abdel-Hamid MI, El-Sherbiny IM. Preparation of silver nanoparticles in the presence of chitosan by electrochemical method. *Carbohydr Polym*. 2012;89(1):236–244.
30. Nasretdinova GR, Fazleeva RR, Mukhitova RK, et al. Electrochemical synthesis of silver nanoparticles in solution. *Electrochem Commun*. 2015;50:69–72.
31. Lai YK, Zhuang HF, Xie KP, et al. Fabrication of uniform Ag/TiO_2 nanotube array structures with enhanced photoelectrochemical performance. *New J Chem*. 2010;34(7):1335–1340.
32. Zaarour M, El Roz M, Dong B, et al. Photochemical preparation of silver nanoparticles supported on zeolite crystals. *Langmuir*. 2014;30(21):6250–6256.
33. Paladini F, Picca RA, Sportelli MC, Cioffi N, Sannino A, Pollini M. Surface chemical and biological characterization of flax fabrics modified with silver nanoparticles for biomedical applications. *Mater Sci Eng C*. 2015;52:1–10.
34. Elsupikhe RF, Shameli K, Ahmad MB. Sonochemical method for the synthesis of silver nanoparticles in j-carrageenan from silver salt at different concentrations. *Res Chem Intermediat*. 2015;41(11):8515–8525.
35. Elsupikhe RF, Shameli K, Ahmad MB, Ibrahim NA, Zainudin N. Green sonochemical synthesis of silver nanoparticles at varying concentrations of κ-carrageenan. *Nanoscale Res Lett*. 2015;10:302.
36. Darroudi M, Zak AK, Muhamad MR, Huang NM, Hakimi M. Green synthesis of colloidal silver nanoparticles by sonochemical method. *Mater Lett*. 2012;66(1):117–120.
37. Pandey JK, Swarnkar RK, Soumya KK, et al. Silver nanoparticles synthesized by pulsed laser ablation: as a potent antibacterial agent for human enteropathogenic gram-positive and gram-negative bacterial strains. *Appl Biochem Biotechnol*. 2014;174(3):1021–1031.
38. Mendivil MI, Krishnan B, Sanchez FA, et al. Synthesis of silver nanoparticles and antimony oxide nanocrystals by pulsed laser ablation in liquid media. *Appl Phys A*. 2013;110(4):809–816.
39. Li SH, Huang JY, Ge MZ, et al. Robust flower-like TiO_2@cotton fabrics with special wettability for effective self-cleaning and versatile oil/water separation. *Adv Mater Interfaces*. 2015;2(14):1500220.
40. Huang JY, Li SH, Ge MZ, et al. Robust superhydrophobic TiO_2@fabrics for UV shielding, self-cleaning and oil-water separation. *J Mater Chem A*. 2015;3(6):2825–2832.
41. Peng LH, Guo RH, Lan JW, Jiang SX, Lin SJ. Microwave-assisted deposition of silver nanoparticles on bamboo pulp fabric through dopamine functionalization. *Appl Surf Sci*. 2016;386:151–159.
42. Rehan M, Mashaly HM, Mowafi S, EI-Kheir AA, Emam HE. Multifunctional textile design using in-situ Ag NPs incorporation into natural fabric matrix. *Dyes Pigments*. 2015;118:9–17.
43. Milošević M, Radoičić M, Šaponjić Z, et al. In situ photoreduction of Ag^+-ions by TiO_2 nanoparticles deposited on cotton and cotton/PET fabrics. *Cellulose*. 2014;21(5):3781–3795.
44. Milošević M, Krkobabić A, Radoičić M, et al. Antibacterial and UV protective properties of polyamide fabric impregnated with TiO_2/Ag nanoparticles. *J Serb Chem Soc*. 2015;80(5):705–715.
45. Rai M, Yadav A, Gade A. Silver nanoparticles as a new generation of antimicrobials. *Biotechnol Adv*. 2009;27(1):76–83.
46. Zhang S, Tang YA, Vlaholic B. A review on preparation and applications of silver-containing nanofibers. *Nanoscale Res Lett*. 2016;11:80.
47. Yu M, Wang ZQ, Lv M, et al. Antisuperbug cotton fabric with excellent laundering durability. *ACS Appl Mater Interfaces*. 2016;8(31):19866–19871.
48. Rana M, Hao B, Mu L, Chen L, Ma PC. Development of multi-functional cotton fabrics with Ag/AgBr-TiO_2. *Compos Sci Technol*. 2016;122:104–112.

Supplementary materials

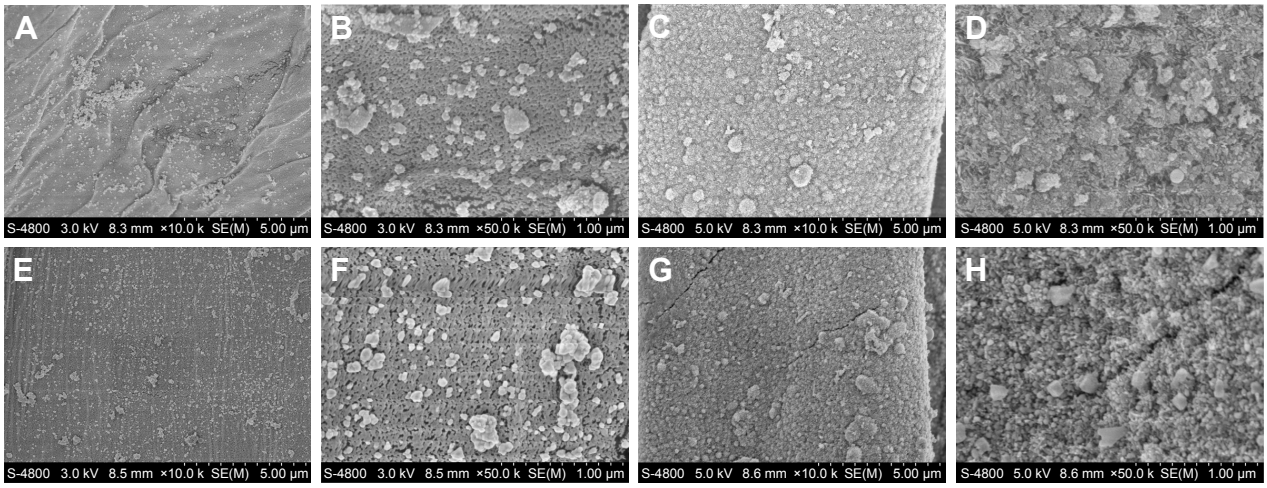

Figure S1 High-resolution SEM images of coated cotton fabrics.
Notes: AgC-6.25 (**A**, **B**), AgTiC-6.25 (**C**, **D**), AgC-25 (**E**, **F**), and AgTiC-25 (**G**, **H**).
Abbreviation: SEM, scanning electron microscopy.

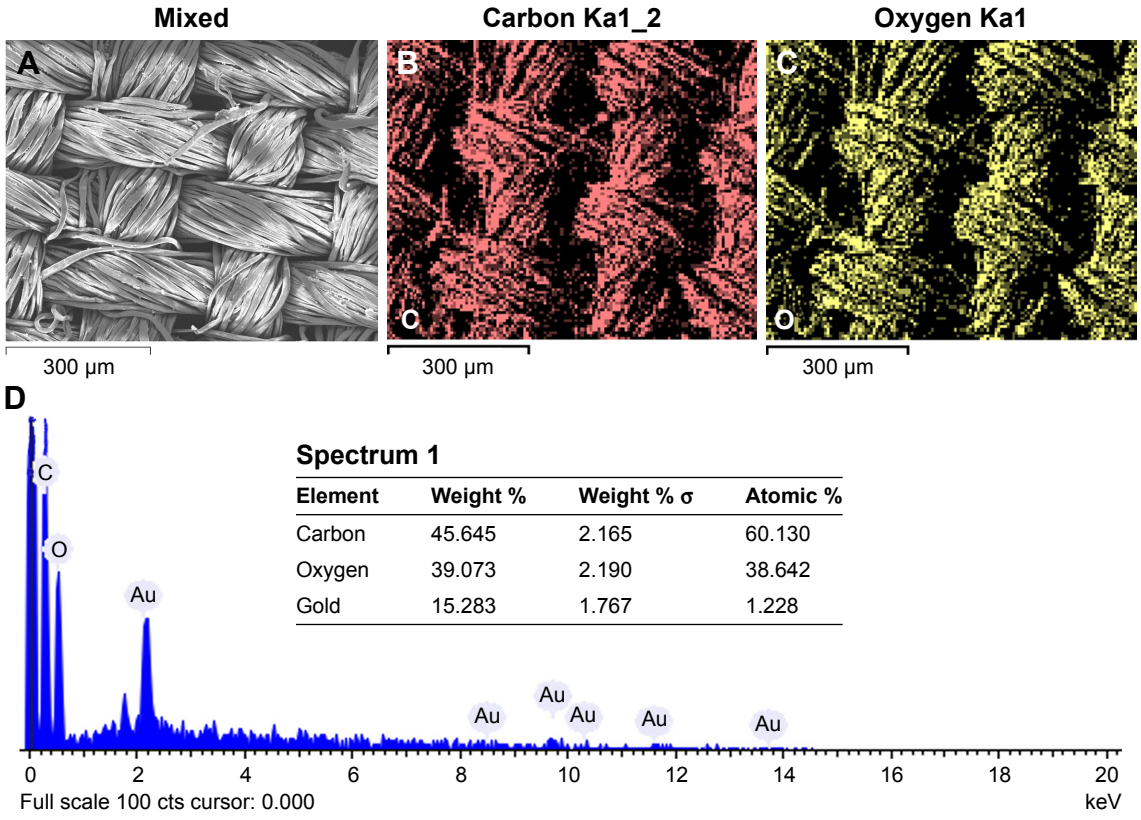

Figure S2 Elements mapping (**A**–**C**) and the energy spectrum and elements proportion (**D**) of pristine cotton surface.
Abbreviations: C, carbon element; O, oxygen element.

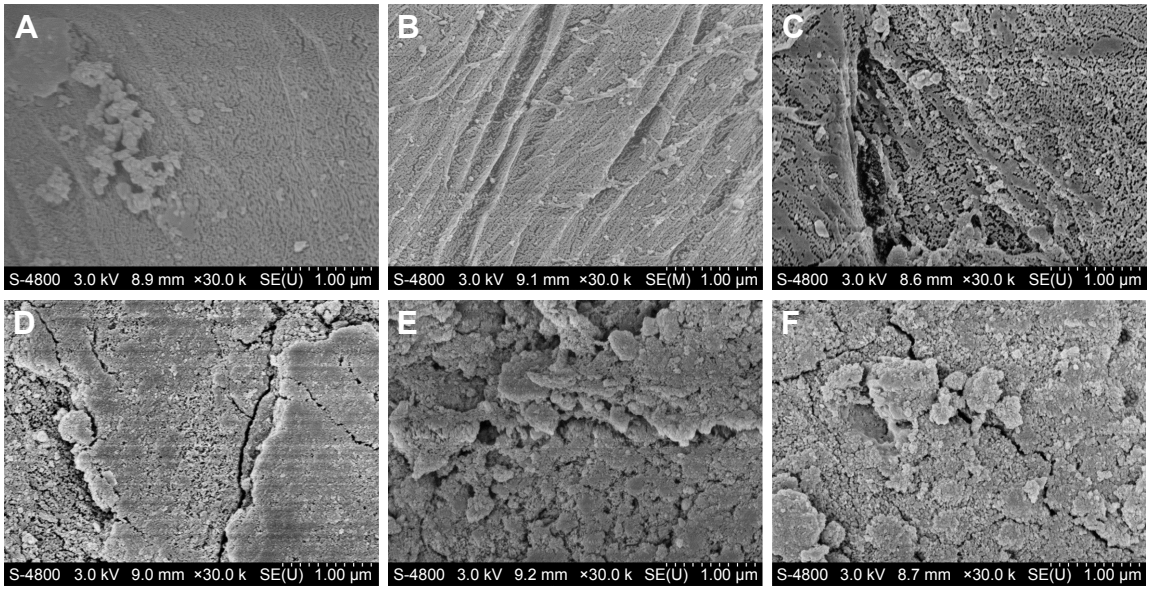

Figure S3 The SEM images of various coated cotton surfaces after laundering for 50 commercial cycles.
Notes: AgC-6.25 (**A**), AgC-25 (**B**), AgC-25 (**C**), AgTiC-6.25 (**D**), AgTiC-25 (**E**), and AgTiC-25 (**F**).
Abbreviation: SEM, scanning electron microscopy.